DIGITALCOMMONS
@WAYNESTATE

Wayne State University

Human Biology Open Access Pre-Prints

WSU Press

4-16-2024

Investigation Of The Prevalence Of IFITM3 Polymorphisms (rs12252 and rs34481144) In Turkish Population: A Pilot Study And Survey Conducted During The COVID-19 Pandemic

Dilek Pirim
Uludag University, dilekpirim@uludag.edu.tr

Fatih Atilla Bağcı
Bursa Uludag University

Hasan Faruk Niş
Bursa Uludag University

Emin Halis Akalın
Bursa Uludag University

Follow this and additional works at: https://digitalcommons.wayne.edu/humbiol_preprints

Recommended Citation

Pirim, Dilek; Bağcı, Fatih Atilla; Niş, Hasan Faruk; and Akalın, Emin Halis, "Investigation Of The Prevalence Of IFITM3 Polymorphisms (rs12252 and rs34481144) In Turkish Population: A Pilot Study And Survey Conducted During The COVID-19 Pandemic" (2024). *Human Biology Open Access Pre-Prints*. 212.
https://digitalcommons.wayne.edu/humbiol_preprints/212

This Article is brought to you for free and open access by the WSU Press at DigitalCommons@WayneState. It has been accepted for inclusion in Human Biology Open Access Pre-Prints by an authorized administrator of DigitalCommons@WayneState.

Investigation Of The Prevalence Of *IFITM3* Polymorphisms (rs12252 and rs34481144) In Turkish Population: A Pilot Study And Survey Conducted During The COVID-19 Pandemic

Dilek Pirim[1,2], Fatih Atilla Bağcı[3], Hasan Faruk Niş[3], Emin Halis Akalın[4]

[1] Bursa Uludag University, Faculty of Arts & Science, Department of Molecular Biology and Genetics, Bursa, Türkiye

[2] Bursa Uludag University, Institute of Health Sciences, Department of Translational Medicine, Bursa, Türkiye

[3] Bursa Uludag University, Institute of Natural and Applied Sciences, Department of Molecular Biology and Genetics, Bursa, Türkiye

[4] Bursa Uludag University, Faculty of Medicine, Department of Infectious Diseases and Clinical Microbiology, Bursa, Türkiye

*Corresponding author: Assoc. Prof. Dilek Pirim, Ph.D., Bursa Uludag University, Department of Molecular Biology and Genetics, Department of Translational Medicine, Bursa, Türkiye E-mail: dilekpirim@uludag.edu.tr

Keywords: *IFITM, IFITM3*, rs12252, rs34481144, SNPs, COVID-19

Short title: *Screening of IFITM3 SNPs in Turkish population*

Abstract Interferon-induced Transmembrane Protein 3 (*IFITM3*) plays a substantial role in the immune system by repressing viral entry into host cells and restricting virus replication. Recent research suggests that *IFITM3*/rs34481144 and *IFITM3*/rs12252 contribute to susceptibility to viral infections across populations dependent on their population frequencies, which needs further clarification. Here, we conducted a population-based study to determine the prevalence of two regulator SNPs in the Turkish population and evaluated genotype and allele frequencies in individuals stratified into groups based on a pilot survey conducted during the COVID-19 pandemic. The Tetra-Primer Arms PCR (TPA-PCR) assays and Sanger sequencing methods were used for genotyping rs34481144 and rs12252, and all participants (n=200) participated in a questionnaire consisting of items related to individual experiences during COVID-19 pandemic. Distributions of genotype frequencies and pairwise linkage disequilibrium (LD) correlations were calculated and compared to publicly available data from worldwide populations. The frequency of minor alleles of rs12252-G and rs34481144-T were found to be 0.128 and 0.324, respectively, in the total sample. Our preliminary data obtained from a self-reported survey gave no concrete evidence for the correlation of the analyzed SNPs with COVID-19 severity or vaccine side effects yet pinpointed a trend for an association of rs12252-G with symptom burdens which requires further investigation. Overall, our results present genotype and allele distributions of two *IFITM3* polymorphisms in the Turkish population and provide present preliminary data on the previously propounded correlations of the genotypes with COVID-19 in our population.

Preprint version. Visit http://digitalcommons.wayne.edu/humbiol/ after publication to acquire the final version.

Interferons (IFNs) are types of cytokine, a class of inflammatory molecules, released from cells in response to pathogen attacks and play a pivotal role in the host defense system (Negishi et al., 2018, Gómez-Herranz et al., 2023). The secretion of IFNs initiates the expression of genes called interferon-stimulating genes (ISGs), which encode proteins exerting critical antiviral properties and lead to viral replication inhibition (Diamond et al., 2013, Liao et al., 2019, Schoggins, 2019). Interferon-induced transmembrane proteins (IFITMs) are known to be fundamental ISG products localized in plasma and endolysosomal membranes that restrain viral entry and hinder pathogen infectivity (Yánez et al., 2020, Liao et al., 2019, Bailey et al., 2014). Accumulating evidence shows that IFITMs also contribute to crucial pathways involving cell cycle control and apoptosis. Thus, dysregulated IFITM proteins not only influence host immune response but are also found to be associated with distinct complex pathologies such as cancer development, Alzheimer's disease, and even with the fetal growth abnormalities (Liu et al., 2019, Xu and Liu, 2023, Lee et al., 2020, Rajapaksa et al., 2020, Buchrieser et al., 2019). The *IFITM3* gene is one of the important members of the *IFITM* gene cluster and spans a region of approximately 18kb on chromosome 11 in humans (Yánez et al., 2020, Liao et al., 2019, Jia et al., 2015). The antiviral proteins encoded by the *IFITM* gene family are considered major players in the innate immune system by suppressing viral propagation of SARS coronavirus, HIV-1, dengue virus, tick-borne encephalitis virus, and influenza A virus (IAV) (Zhao et al., 2018, Brass et al., 2009, Huang et al., 2011, Wrensch et al., 2014, Prelli Bozzo et al., 2021, Chmielewska et al., 2022, Feeley et. al., 2011, Lu et al., 2011, Hachim et al., 2020). Hence, characterizing *IFITMs* DNA sequence variants and unraveling their impacts on the chain of transmission is of utmost importance and an attractive research field for researchers, especially after experiencing the devastating global COVID-19 pandemic.

A considerable amount of research has been conducted to investigate the associations of the genetic variants in the *IFITM3* with infectious disease. To date, two functional variants (rs12252 and rs34481144) are the most widely studied *IFITM3* single nucleotide polymorphisms (SNPs) that have been suggested to be associated with human viral infections in different ethnic populations (Pati et al., 2021, Allen et al., 2017, Gómez et al., 2021, Nikoloudis et al., 2020, Mohammed et al., 2021, Kim and Jeong 2020b, Leandro et al., 2023, Martins et al., 2020). The rs34481144 is located in the promoter of the *IFITM3* and the rs34481144-A allele was shown to diminish the antiviral function of the IFITM3 protein by preventing intact binding of transcription factors (Allen et al., 2017). However, the rs12252-GG genotype was shown to result in truncated protein causing detrimental functional consequences (Mohammed et al., 2021, Everitt et al., 2012, Makvandi-Nejad et al., 2018). Few studies also investigated the associations

of these SNPs with immune response after vaccination against COVID-19 and influenza but results are inconclusive and need clarification (Čiučiulkaitė et al., 2023, Lei et al., 2020). Moreover, multiple studies implicate the associations of the less frequent allele (G) of rs12252 with the HIV progression, influenza severity, risk, and severity of COVID-19 in Chinese and Spanish populations, yet inconclusive results were also obtained from studies recruiting samples from distinct ancestry (Zheng et al., 2020, Zhang et al., 2013, Zhang et al., 2019, Gómez et al., 2021, Mills et al., 2014, López-Rodríguez et al., 2016, Randolph et al., 2017, Schönfelder et al., 2021, Martins et al., 2020). Likewise, the association of the functional *IFITM3*/rs34481144 with viral infections has been reported in studies including specific populations and therefore suggested associations remain elusive for unrepresented populations with different allele distributions (Kim and Jeong 2020a, Pati et al., 2021).

Considering the published literature, two functional variants of *IFITM3* may contribute to the pathogenesis of viral infections so elucidating their prevalence in diverse populations may provide population-specific information for managing and surveilling viral diseases. In light of this objective, we conducted a pilot study to screen rs12252 and rs34481144 in the Turkish population and also gathered information about the COVID-19 experiences of the individuals who participated in our research.

MATERIALS & METHODS

Samples

Two hundred individuals (123 Females, 77 Males) aged ≥18 years from the general population participated in our study between May 2022 and February 2023. All protocols were practiced with the approval of the Institutional Review Board (IRB) of the Bursa Uludag University (2022–8/35). Each participant gave informed consent before sample collection and was asked to fill out a questionnaire form about experiences of the COVID-19 pandemic and their symptoms of SARS-CoV-2 infection. Participants were stratified into groups based on the responses related to COVID-19 RT-PCR test status, symptoms, and post-vaccine reactions. Two ml of saliva samples were collected in Saliva Collection Tubes (Hibrigen, Türkiye) and stored at -20°C until DNA isolation.

DNA isolation

Saliva samples collected in saliva collection tubes were used for genomic DNA isolation. Five

hundred µL saliva samples were treated by proteinase K and incubated for 3 hours at 56 ˚C before DNA isolation. Genomic DNA was isolated using the Saliva DNA Extraction Kit (Hibrigen, Türkiye) by modifying the protocol with additional spin-column purification steps (PureLink Spin Columns, Thermo Fisher Scientific). DNA yield and quality were measured for quantity and quality in NanoDrop 2000 (Thermo Fisher Scientific) and Qubit 4.0 (Thermo Fisher Scientific). An average of 102.6 ng/µL genomic DNA was extracted from saliva samples and adjusted to 10 ng/µL for PCR reactions.

Genotyping

Tetra-primer ARMS PCR (TPA-PCR) assays were designed for SNP genotyping (Medrano & de Oliveira, 2014) and genotypes were confirmed by Sanger Sequencing. Primers used in Tetra-Primer ARMS PCR were designed by using online bioinformatic tools (Primer 1 (http://primer1.soton.ac.uk/primer1.html) and listed in Supplementary Table 1. For the rs12252; 1.3 µL DNA (10 ng/µL), 1.25 µL 10x PCR Buffer, 0.7 µL MgCl2 (25 mM), 0.2 µL of outer primers (10 µM), 0.15 µL forward inner primer (10 µM), 0.2 µL reverse inner primer (10 µM), 0.25 µL dNTP (10mM), 8.175 µL of nuclease-free water, 0.075 µL Taq polymerase (AmpliTaq Polymerase, Thermo Fisher Scientific) were used in a final volume of 12.5 µL. For the rs34481144; 1 ul DNA (10 ng/µL), 1.25 µL 10x PCR Buffer, 1 µL MgCl2 (25 mM), 0.25 µL of outer primers (10 µM), 0.25 µL of inner primers (10 µM), 0.25 µL dNTP (10mM), 7,925 µL of nuclease-free water, 0.075 µL Taq polymerase (AmpliTaq Polymerase, Thermo Fisher Scientific) were used in a final volume of 12.5 µL. All PCR reactions were performed in the SimpliAmp Thermal Cycler (Thermo Fisher) with conditions given in Supplementary Table 2. PCR products were visualized in 3 % agarose gel electrophoresis and genotypes were recorded as Wild Type, Homozygote, and Heterozygote. Genotypes were confirmed by Sanger Sequencing on the Applied Biosystems DNA Analyzers by sequencing primers (Forward: GCGGCACCCTCTGAGCATT, Reverse: AAGATGAGCCTTGTGCTCCC) targeting the 536bp sequence of the *IFITM3* gene harboring rs12252 and rs34481144. PCR conditions are provided in Supplementary Table 3.

Statistical and Bioinformatics analysis

Haploview software was used to calculate the Hardy-Weinberg Equilibrium (HWE) *p*-value and pairwise linkage disequilibrium (LD) measure of the SNPs. The distributions of the genotypes in stratified groups defined by COVID-19 experiences were also assessed by a chi-square test

conducted in Haploview software (Barrett et al., 2005). Sequence chromatograms were analyzed by using the Sequencher (Gene Codes, Ann Harbor, MI) and BioEdit software. We also used the LDlink online tool to assess the pairwise LD measure and genotype distributions of the two variants in the worldwide populations (https://ldlink.nih.gov/?tab=home) (accessed 5 August 2023). Regulatory and eQTL properties of the two SNPs were retrieved from the RegulomeDB and Genotype-Tissue Expression (GTEx) databases (Boyle et al., 2012). A *p*-value of less than 0.05 is considered a statistically significant result.

RESULTS

Characteristics of the study subjects and their experiences during the COVID-19 pandemic

Of 200 individuals, 69 (34.5 %) declared not to take any RT-PCR COVID-19 test since they never felt any symptoms or contact with a COVID-19-positive individual, 65 (32.5 %) tested negative and 66 (33 %) had a positive COVID-19 test at the time of the interview. Of 66 individuals who tested positive, 35 were diagnosed with COVID-19 before the first vaccine administration, and 16 were diagnosed with COVID-19 both before and after vaccine administration. However, 51 individuals (pre-vaccine COVID-19 disease) experienced at least one COVID-19 symptom among 12 symptoms included in the questionnaire, and 56.86 % of these individuals (n=29) had >6 symptoms (Table 3). Of note, only three individuals were reported to be hospitalized due to severe COVID-19 infection. One ninety-three individuals received one of the COVID-19 vaccines (Pfizer-BiNoTech, SinoVac, Turkovac, Moderna) at least one dose, and 73.5 % (n=147) of the responders took the Pfizer-BioNTech mRNA vaccine. Moreover, 104 individuals developed local adverse (n=14) and/or systematic reactions (n=25) after Pfizer-BioNTech COVID-19 vaccine administration. The characteristics of the samples are presented in Supplementary Table 4.

Allele frequency distributions of the IFITM3/rs12252 and IFITM3/rs3448114

All genotypes were found to be in Hardy-Weinberg equilibrium (HW-*p*-value>0.05). One hundred eighty-four and one hundred eighty-eight individuals were successfully genotyped for rs12252 and rs3448114, respectively. Genotypes were confirmed by Sanger sequencing and chromatograms showing the genotypes of two SNPs were given in Fig. 1. Both SNPs had

common minor allele frequencies (MAF) values in our sample of which the minor allele of rs3448114-T (MAF=0.324) was seen more frequently compared to rs12252-G (MAF=0.128). Table 1 shows distributions of the allele frequencies of the rs12252 and rs3448114 in our sample and results of large-scale population sequencing projects (1000G, EXACT, FINRISK, and TOPMED). Based on the data extracted from the LDlink website, the allele frequency ranges for rs12252-G and rs3448114-T was 0.011–0.6394 and 0–0.5604, respectively, in 31 populations (Table 2 and Fig. 2a-b). We also analyzed the distribution of the genotypes in individuals stratified based on their responses in the questionnaire. First, we grouped the individuals who reported having a positive COVID-19 test (pre-vaccination) based on the number of symptoms they experienced during infection. The minor allele (G) frequency of the rs12252 was 0.10 in individuals who had >6 COVID-19 symptoms (Group 1), while a MAF of 0.05 was obtained for rs12252 in individuals with ≤6 symptoms or no symptoms (Group 2) (Table 3). On the other hand, the minor allele (T) frequency of the rs3448114 was similar in the two groups. We also grouped individuals based on their post-vaccination reactions after the Pfizer-BioNTech administration; individuals receiving Sinovac, Turkovac, and Moderna were excluded due to the small sample size. Of 104 individuals who were reported to experience adverse reactions after Pfizer-BioNTech COVID-19 vaccine administration (Group 4), 12.5 % and 32 % had rs12252-G and rs3448114-T alleles, respectively. Allele frequencies were 12.8 % and 28.7 % for rs12252-G and rs3448114-T, respectively, in individuals reporting no Pfizer-BioNTech adverse reaction (Group 3) (Table 4). Distributions of SNPs in groups of individuals experiencing local (n=14, Group 5) and systematic adverse reactions (n=25, Group 6) after Pfizer-BioNTech administration were also analyzed and presented in Table 4. Additionally, pairwise LD between rs12252 and rs3448114 was measured by using Haploview software and no correlation (r^2 =0.017) was obtained between allele frequencies of the tested SNPs. We also determined the pairwise LD correlation of the two SNPs in other populations included in the 1000 Genome Project and, similarly, there was no significant pairwise LD (r^2 =0.0862–0.0027) between them in distinct populations (Fig. 3 and Table 2).

Functional Annotations of the *IFITM3*/rs12252 and *IFITM3*/rs3448114

RegulomeDB and GTEx databases were used to evaluate the functional impact of the two SNPs. Both SNPs were found to have a RegulomeDB score of 1f indicating they are located in a site that may affect transcription factor binding and have eQTL properties (Supplementary Table 5).

Based on the data retrieved from the GTEx database, both SNPs can affect the expressions of multiple genes in different tissues (Supplementary Table 5). We found that rs34481144 is an eQTL SNP that affects *IFITM3* and other genes in the *IFITM* gene family in 45 tissues such as the lung, whole blood, heart, ovary, pancreas, etc. However, rs12252 was identified to affect two genes (*PGGHG, RP11*) in specific tissues (lung, frontal cortex (BA9), muscle (skeletal), adipose (subcutaneous), skin (sun-exposed), nerve (tibial), and whole blood).

DISCUSSIONS

Previous studies have shown that SNPs in the *IFITM3* gene may be predisposing factors for the development and severity of viral infections such as SARS-CoV-2 (Alghamdi et al., 2021, Everitt et al., 2012, Li et al., 2022, Mohammed et al., 2021, Guo et al., 2023). Results obtained from genetic association studies provide promising evidence of the role of *IFITM3* gene polymorphisms in infectious disease management. However, more research, including diverse population-based samples, is needed to clarify their functionality and translational utilization for risk assessments of viral infections. This study aimed to unravel the population-specific allele frequency distribution and allele correlations of the two *IFITM3* SNPs with functional relevance. Consistent with the literature, two SNPs were observed with relatively high frequencies (MAF≥ 0.1) in our population-based sample. Notably, the genotype and allele frequencies of rs12252 and rs34481144 are considerably diverse in populations around the world (Kim and Jeong, 2020a). It has been shown that European, American, and South Asian populations carry rs12252 (GG genotype) with low frequencies compared to African and East Asian populations (Kim and Jeong, 2020a). Populations from Italy, Britain, Finland, Spain, Americans with Northern and Western European Ancestry (CEU population), and Columbia have the lowest allele frequency (<10%) for rs12252-G among all populations in the 1000 Genome Project, while populations from China and Japan have the highest allele frequency (>50 %) for rs12252-G (Table 2, Fig. 2). The frequencies of the rs12252-G and rs34481144-T alleles in Puerto Ricans [rs12252 (G: 0.11), rs34481144 (T: 0.29)] were found to be similar to allele frequencies identified in our study. Meanwhile, rs34481144-T were not detected in populations from China and Japan and higher allele frequencies (>10 %) for rs34481144-T were mostly observed in populations from Europe (Table 2, Fig. 2). Meanwhile, the low pairwise LD between the rs12252 and rs34481144 showed that they were not correlated in populations around the globe (Table 2 and Fig. 3). We also assessed the functional relevance of two SNPs by using RegulomeDB and GTEx databases. The GTEx data showed that expressions of the *PGGHG* and *RP11–326C3* genes are regulated by

rs12252 in lung tissue (Supplementary Table 5). Previously, *PGGHG* was reported to be downregulated in the lung tissues of COVID-19 patients compared to healthy controls (Wu et al. 2020). Also, rs34481144 is found to have possible functional role in regulating multiple genes, such as *PGGHG, IFITM1*, and *IFITM3*, that have implications in immune system related pathologies (Wu et al. 2020, Regino-Zamarripa et al. 2022).

Our study was conducted during the COVID-19 pandemic so we also intended to evaluate participants' experiences of the COVID-19 pandemic by self-report survey. Our survey consists of 12 questions requiring responses related to their COVID-19 infection and COVID-19 vaccination status as well as their symptoms in the course of the disease or post-vaccination period. Thus, we evaluated the genotype distributions and frequencies in a stratified group of individuals based on their responses to the questionnaire. We grouped the individuals according to the number of symptoms (symptom burden) experienced during COVID-19 infections, the status of post-vaccination COVID-19 infection, and the side effects of COVID-19 vaccination. Up to date, limited research exists for understanding the contributions of genetic factors to interindividual reactions caused by COVID-19 vaccines (Bolze et al., 2022a, Bolze et al., 2022b, Čiučiulkaitė et al., 2023). Bolze et al., (2022b) addressed the association of HLA-A∗03:01 with developing stronger side effects after receiving Pfizer-BioNTech COVID-19 vaccinations. We also analyzed our data to see the distributions of alleles in groups stratified based on the reactions developed after the Pfizer-BioNTech COVID-19 vaccine administration. Even though no definite conclusion can be drawn from our pilot study, it is highly recommended that associations of these SNPs with vaccine side effects be clarified in future studies.

Previously, the rs12252-G was associated with the severity of COVID-19 infection, risk of hospitalization, and death in studies recruiting hospitalized patients from China and Spain (Zhang et al., 2019, Gómez et al., 2021). Similar findings were reported in a study conducted in COVID-19 patients of Saudi Arabian descent (n=880) of which rs12252-G was reported to be associated with hospitalization and mortality (Alghamdi et al., 2021). A previous study also reported an association of rs12252-G with severe influenza in Chinese individuals (Zhang et al., 2013). In our study, the minor rs12252-G had a relatively similar MAF in Group 2 (individuals reporting to have ≤6 symptoms during COVID-19 infection, MAF=5 %) and Group 1 (individuals with >6 symptoms, MAF=10 %) (Table 3). Acknowledging our small sample size, we suspect our preliminary findings provide suggestive evidence for the possible association of rs12252-G with the symptom burden of COVID-19 infection in our population, yet more studies need to be conducted to prove this information. However, contradictory results exist in the literature as no association was observed between rs12252-G and COVID-19 infection risk in the

German cohort (Schönfelder et al., 2021). Likewise, the German study failed to exhibit an association between rs34481144-T and COVID-19 severity (Schönfelder et al., 2021). Public data retrieved from the 1000 Genome project revealed the prevalence of the rs34481144 alleles is highly variable among populations from distinct geographies. In a recent study conducted in Iran, rs34481144 was reported to be associated with COVID-19 mortality (Gholami et al., 2023). The study samples consist of 1,149 deceased and 1,342 recovered COVID-19 patients and the rs34481144-TT genotype was found to increase the risk of developing severe COVID-19 infection. Yet, the association of rs34481144 with COVID-19 infection needs clarification in future studies due to the conflicting results reported in the literature (Schönfelder et al., 2021). However, in a case-control study conducted using samples (n=666) with European ancestry (Austria and Northern Spain), rs12252-G and rs34481144-T were found to pose a risk for COVID-19 infection (Cuesta-Llavona et al., 2021).

Interestingly, the data analysis conducted by Pati et al. (2021) yielded an inverse correlation between rs12252-GG and COVID-19 death rates. The study analyzed worldwide COVID-19 death rates and genotype distributions of rs12252 and rs34481144 in 21 countries. In contrast to previous findings, rs12252-G was found to be negatively correlated with COVID-19 mortality rates (Pati et al., 2020). Yet, the correlation of rs34481144 with COVID-19 infection was not reported in their study due to limited worldwide data. Moreover, few studies found a correlation between rs34481144-T and severe outcomes for influenza infection (Allen et al., 2017, Eisfeld and Kawaoka, 2017). We did not have sufficient data to assess the correlations of SNPs with COVID-19 mortality or hospitalization (only 3 individuals reported being hospitalized due to severe symptoms), however, we observed a possible trend for an association of rs12252-G with high symptom burden (Table 3).

To the best of our knowledge, this is the first study that aims to explore the population frequency and distributions of the rs12252 and rs34481144 in Turkey and the result of this pilot study highlights the significance of validation of genetic association findings in distinct populations with diverse allele distributions. However, analyzing the distribution of the SNPs in a larger sample from our population will confer more representative data regarding allele frequencies.

In conclusion, this study presents frequency distributions of two *IFITM3* polymorphisms in the Turkish population and provide preliminary data of the propounded correlations of the genotypes with COVID-19 disease in our population. Results of our pilot study yield promising information for the possible associations of rs12252 with the symptom burden of COVID-19 which needs to be clarified by case-control studies. Unraveling the associations of *IFITM3*

variants with susceptibility and severity of infectious diseases in larger cohorts from populations with distinct genetic backgrounds has the potential to provide promising results for developing translational medicine applications against viral diseases.

REFERENCES

Alghamdi J, Alaamery M, Barhoumi T, et al. Interferon-induced transmembrane protein-3 genetic variant rs12252 is associated with COVID-19 mortality. *Genomics*. 2021;113(4):1733–1741.

Allen EK, Randolph AG, Bhangale T, et al. SNP-mediated disruption of CTCF binding at the IFITM3 promoter is associated with risk of severe influenza in humans. *Nat Med*. 2017;23(8):975–983.

Bailey CC, Zhong G, Huang IC, Farzan M. IFITM-Family Proteins: The Cell's First Line of Antiviral Defense. *Annual Review of Virology*. 2014;1(1):261–283.

Barrett JC, Fry B, Maller J, Daly MJ. Haploview: analysis and visualization of LD and haplotype maps. *Bioinformatics*. 2005;21(2):263–265.

Bolze A, Mogensen TH, Zhang SY, et al. Decoding the Human Genetic and Immunological Basis of COVID-19 mRNA Vaccine-Induced Myocarditis. *J Clin Immunol*. 2022;42(7):1354–1359.

Bolze A, Neveux I, Schiabor Barrett KM, et al. HLA-A∗03:01 is associated with increased risk of fever, chills, and stronger side effects from Pfizer-BioNTech COVID-19 vaccination. *HGG Adv*. 2022;3(2):100084.

Boyle AP, Hong EL, Hariharan M, et al. Annotation of functional variation in personal genomes using RegulomeDB. *Genome Res*. 2012;22(9):1790–1797.

Brass AL, Huang IC, Benita Y, et al. The IFITM Proteins Mediate Cellular Resistance to Influenza A H1N1 Virus, West Nile Virus, and Dengue Virus. *Cell*. 2009;139(7):1243–1254.

Buchrieser J, Degrelle SA, Couderc T, et al. IFITM proteins inhibit placental syncytiotrophoblast formation and promote fetal demise. *Science*. 2019;365(6449):176–180.

Chmielewska AM, Gómez-Herranz M, Gach P, et al. The Role of IFITM Proteins in Tick-Borne Encephalitis Virus Infection. *Journal of Virology*. 2022;96(1):e01130–21.

Čiučiulkaitė I, Siffert W, Elsner C, et al. Influence of the Single Nucleotide Polymorphisms rs12252 and rs34481144 in IFITM3 on the Antibody Response after Vaccination against COVID-19. *Vaccines*. 2023;11(7):1257.

Cuesta-Llavona E, Albaiceta GM, García-Clemente M, et al. Association between the interferon-induced transmembrane protein 3 gene (*IFITM3*) rs34481144 / rs12252 haplotypes and COVID-19. *Curr Res Virol Sci*. Published online 2021:100016–100016.

Diamond MS, Farzan M. The broad-spectrum antiviral functions of IFIT and IFITM proteins. *Nat Rev Immunol*. 2013;13(1):46–57.

Eisfeld AJ, Kawaoka Y. Calculated Risk: A New SNP Linked to Severe Influenza Disease. *Nat Med*. 2017;23(8):911–912.

Everitt AR, Clare S, Pertel T, et al. IFITM3 restricts the morbidity and mortality associated with influenza. *Nature*. 2012;484(7395):519–523.

Feeley EM, Sims JS, John SP, et al. IFITM3 Inhibits Influenza A Virus Infection by Preventing Cytosolic Entry. *PLOS Pathogens*. 2011;7(10):e1002337.

Gholami M, Sakhaee F, Mirzaei Gheinari F, et al. Interferon-Induced Transmembrane Protein 3 rs34481144 C/T Genotype and Clinical Parameters Related to Progression of COVID-19. *Journal of Immunology Research*. 2023;2023:e2345062.

Gómez J, Albaiceta GM, Cuesta-Llavona E, et al. The Interferon-induced transmembrane protein 3 gene (IFITM3) rs12252 C variant is associated with COVID-19. *Cytokine*. 2021;137:155354.

Gómez-Herranz M, Taylor J, Sloan RD. IFITM proteins: Understanding their diverse roles in viral infection, cancer, and immunity. *Journal of Biological Chemistry*. 2023;299(1):102741.

Guo H, Zhao T. Multiple mutations of IFITM3 are associated with COVID-19 susceptibilityregulation function of IFITM3 in COVID-19. *J Infect*. 2023;86(6):614–616.

Hachim MY, Al Heialy S, Hachim IY, et al. Interferon-Induced Transmembrane Protein (IFITM3) Is Upregulated Explicitly in SARS-CoV-2 Infected Lung Epithelial Cells. *Front Immunol*. 2020;11:1372.

Huang IC, Bailey CC, Weyer JL, et al. Distinct patterns of IFITM-mediated restriction of filoviruses, SARS coronavirus, and influenza A virus. *PLoS Pathog*. 2011;7(1):e1001258.

Jia R, Ding S, Pan Q, Liu SL, Qiao W, Liang C. The C-terminal sequence of IFITM1 regulates its anti-HIV-1 activity. *PLoS One*. 2015;10(3):e0118794.

Kim YC, Jeong BH. Ethnic variation in risk genotypes based on single nucleotide polymorphisms (SNPs) of the interferon-inducible transmembrane 3 (IFITM3) gene, a susceptibility factor for pandemic 2009 H1N1 influenza A virus. *Immunogenetics*. 2020;72(9–10):447–453.

Kim YC, Jeong BH. Strong Correlation between the Case Fatality Rate of COVID-19 and the rs6598045 Single Nucleotide Polymorphism (SNP) of the Interferon-Induced Transmembrane Protein 3 (IFITM3) Gene at the Population-Level. *Genes (Basel)*. 2020;12(1):42.

Leandro DB, Celerino da Silva R, Rodrigues JKF, et al. Clinical-Epidemiological Characteristics and IFITM-3 (rs12252) Variant Involvement in HIV-1 Mother-to-Children Transmission Susceptibility in a Brazilian Population. *Life (Basel)*. 2023;13(2):397.

Lee J, Robinson ME, Ma N, et al. IFITM3 functions as a PIP3 scaffold to amplify PI3K signalling in B cells. *Nature*. 2020;588(7838):491–497.

Lei N, Li Y, Sun Q, et al. IFITM3 affects the level of antibody response after influenza vaccination. *Emerg Microbes Infect*. 2020;9(1):976–987.

Li Y, Wei L, He L, Sun J, Liu N. Interferon-induced transmembrane protein 3 gene polymorphisms are associated with COVID-19 susceptibility and severity: A meta-analysis. *J Infect*. 2022;84(6):825–833.

Liao Y, Goraya MU, Yuan X, Zhang B, Chiu SH, Chen JL. Functional Involvement of Interferon-Inducible Transmembrane Proteins in Antiviral Immunity. *Front Microbiol*. 2019;10:1097.

Liu X, Chen L, Fan Y, et al. IFITM3 promotes bone metastasis of prostate cancer cells by mediating activation of the TGF-β signaling pathway. *Cell Death Dis*. 2019;10(7):517.

López-Rodríguez M, Herrera-Ramos E, Solé-Violán J, et al. IFITM3 and severe influenza virus infection. No evidence of genetic association. *Eur J Clin Microbiol Infect Dis*. 2016;35(11):1811–1817.

Lu J, Pan Q, Rong L, Liu SL, Liang C. The IFITM proteins inhibit HIV-1 infection. *Journal of Virology*. 2011;85(5):2126–2137.

Makvandi-Nejad S, Laurenson-Schafer H, Wang L, et al. Lack of Truncated IFITM3 Transcripts in Cells Homozygous for the rs12252-C Variant That is Associated With Severe Influenza Infection. *J Infect Dis*. 2018;217(2):257–262.

Martins JSC, Oliveira MLA, Garcia CC, Siqueira MM, Matos AR. Investigation of Human IFITM3 Polymorphisms rs34481144A and rs12252C and Risk for Influenza A(H1N1)pdm09 Severity in a Brazilian Cohort. *Front Cell Infect Microbiol*. 2020;10:352.

Medrano RFV, de Oliveira CA. Guidelines for the tetra-primer ARMS-PCR technique development. *Mol Biotechnol*. 2014;56(7):599–608.

Mills TC, Rautanen A, Elliott KS, et al. IFITM3 and Susceptibility to Respiratory Viral

Infections in the Community. *J Infect Dis*. 2014;209(7):1028–1031.

Mohammed FS, Farooqi YN, Mohammed S. The Interferon-Induced Transmembrane Protein 3 - rs12252 Allele May Predict COVID-19 Severity Among Ethnic Minorities. *Front Genet*. 2021;12:692254.

Negishi H, Taniguchi T, Yanai H. The Interferon (IFN) Class of Cytokines and the IFN Regulatory Factor (IRF) Transcription Factor Family. *Cold Spring Harb Perspect Biol*. 2018;10(11):a028423.

Nikoloudis D, Kountouras D, Hiona A. The frequency of combined IFITM3 haplotype involving the reference alleles of both rs12252 and rs34481144 is in line with COVID-19 standardized mortality ratio of ethnic groups in England. *PeerJ*. 2020;8:e10402.

Pati A, Padhi S, Suvankar S, Panda AK. Minor Allele of Interferon-Induced Transmembrane Protein 3 Polymorphism (rs12252) Is Covered Against Severe Acute Respiratory Syndrome Coronavirus 2 Infection and Mortality: A Worldwide Epidemiological Investigation. *J Infect Dis*. 2021;223(1):175–178.

Prelli Bozzo C, Nchioua R, Volcic M, et al. IFITM proteins promote SARS-CoV-2 infection and are targets for virus inhibition in vitro. *Nat Commun*. 2021;12(1):4584.

Rajapaksa US, Jin C, Dong T. Malignancy and IFITM3: Friend or Foe? *Front Oncol*. 2020;10:593245.

Randolph AG, Yip WK, Allen EK, et al. Evaluation of IFITM3 rs12252 Association With Severe Pediatric Influenza Infection. *The Journal of Infectious Diseases*. 2017;216(1):14–21.

Regino-Zamarripa NE, Ramírez-Martínez G, Jiménez-Álvarez LA, et al. Differential Leukocyte Expression of IFITM1 and IFITM3 in Patients with Severe Pandemic Influenza A(H1N1) and COVID-19. *J Interferon Cytokine Res*. 2022;42(8):430–443.

Schoggins JW. Interferon-Stimulated Genes: What Do They All Do? *Annu Rev Virol*. 2019;6(1):567–584.

Schönfelder K, Breuckmann K, Elsner C, et al. The influence of IFITM3 polymorphisms on susceptibility to SARS-CoV-2 infection and severity of COVID-19. *Cytokine*. 2021;142:155492.

Solé X, Guinó E, Valls J, Iniesta R, Moreno V. SNPStats: a web tool for the analysis of association studies. *Bioinformatics*. 2006;22(15):1928–1929.

Srivastava A, Hollenbach JA. The immunogenetics of COVID-19. *Immunogenetics*. 2023;75(3):309–320.

Wu M, Chen Y, Xia H, et al. Transcriptional and proteomic insights into the host response in

fatal COVID-19 cases. *Proc Natl Acad Sci U S A*. 2020;117(45):28336–28343.

Xu H, Liu Y. ROS-responsive nanomodulators downregulate IFITM3 expression and eliminate ROS for Alzheimer's disease combination treatment. *Journal of Colloid and Interface Science*. 2023;645:210–218.

Yánez DC, Ross S, Crompton T. The IFITM protein family in adaptive immunity. *Immunology*. 2020;159(4):365–372.

Zhang Y, Qin L, Zhao Y, et al. Interferon-Induced Transmembrane Protein 3 Genetic Variant rs12252-C Associated With Disease Severity in Coronavirus Disease 2019. *The Journal of Infectious Diseases*. 2020;222(1):34–37.

Zhang YH, Zhao Y, Li N, et al. Interferon-induced transmembrane protein-3 genetic variant rs12252-C is associated with severe influenza in Chinese individuals. *Nat Commun*. 2013;4(1):1418.

Zhao X, Li J, Winkler CA, An P, Guo JT. IFITM Genes, Variants, and Their Roles in the Control and Pathogenesis of Viral Infections. *Front Microbiol*. 2018;9:3228.

Zheng M, Zhao X, Zheng S, et al. Bat SARS-Like WIV1 coronavirus uses the ACE2 of multiple animal species as receptor and evades IFITM3 restriction via TMPRSS2 activation of membrane fusion. *Emerg Microbes Infect*. 2020;9(1):1567–1579.

TABLES

Table 1. Allele frequency distributions of rs12252 and rs34481144

RefSNP ID	Alleles	Chr loc.[a] (GRCh38.p14)	Location	HW-*p*[b]	Allele Freq[c]	Genotype (n, %)	1000G[d]	ExAC[e]	FINRISK[f]	TOPMed[g]
rs12252	A:G	320772	Exon1 (Ser42Ser)	1.0	A: 87.2 % G: 12.8 %	AA (n=140, 70 %) AG (n=41, 20.5 %) GG (n=3, 1.5 %)	0.23 (n=2504)	0.124 (n=6281)	-	0.14 (n=132345)
rs34481144	C:T	320836	Exon1 (5'UTR)	0.6	C: 67.6% T: 32.4 %	CC (n=88, 44 %) CT (n=78, 39 %) TT (n=22, 11 %)	0.17 (n=2504)	0.37 (n=58862)	0.54 (n=152)	0.30 (n=132345)

a; Chromosomal location on chromosome 11, b; H-W *p*-value, c; Allel Frequency, d; 1000 Genome Project MAF in gobal, e; The Exome Aggregation Consortium (ExAC) MAF in global, f; Finnish from FINRISK project MAF, g; Trans-Omics for Precision Medicine (TOPMed) MAF in global.

Table 2. Allele frequency distributions of rs34481144 and rs12252 in worldwide populations

Population	Abbrev	N	rs12252 Allele Freq	rs34481144 Allele Freq	r^2
Our Population	-	188	A:87.2% G:12.8%	C:67.6%, T:32.4%	0.017
All Populations	ALL	2504	A: 76.36%, G: 23.64%	C: 82.19%, T: 17.81%	0.0671
African	AFR	661	A: 73.98%, G: 26.02%	C: 95.69%, T: 4.31%	0.0158
Yoruba in Ibadan, Nigeria	YRI	108	A: 66.67%, G: 33.33%	C: 96.76%, T: 3.24%	0.0167
Luhya in Webuye, Kenya	LWK	99	A: 70.2%, G: 29.8%	C: 98.48%, T: 1.52%	0.0065
Gambian in Western Divisions in the Gambia	GWD	113	A: 78.32%, G: 21.68%	C: 96.9%, T: 3.1%	0.0088
Mende in Sierra Leone	MSL	85	A: 75.29%, G: 24.71%	C: 98.24%, T: 1.76%	0.0059
Esan in Nigeria	ESN	99	A: 78.79%, G: 21.21%	C: 98.99%, T: 1.01%	0.0027
Americans of African Ancestry in SW USA	ASW	61	A: 69.67%, G: 30.33%	C: 86.07%, T: 13.93%	0.0705
African Caribbeans in Barbados	ACB	96	A: 77.6%, G: 22.4%	C: 90.62%, T: 9.38%	0.0299
Ad Mixed American	AMR	347	A: 82.28%, G: 17.72%	C: 76.66%, T: 23.34%	0.0656
Mexican Ancestry from Los Angeles USA	MXL	64	A: 78.12%, G: 21.88%	C: 82.03%, T: 17.97%	0.0613
Puerto Ricans from Puerto Rico	PUR	104	A: 88.94%, G: 11.06%	C: 70.19%, T: 29.81%	0.0528
Colombians from Medellin, Colombia	CLM	94	A: 92.55%, G: 7.45%	C: 68.09%, T: 31.91%	0.0377
Peruvians from Lima, Peru	PEL	85	A: 65.88%, G: 34.12%	C: 90.0%, T: 10.0%	0.0575

East Asian	EAS	504	A: 47.22%, G: 52.78%	C: 99.4%, T: 0.6%	0.0067
Han Chinese in Beijing, China	CHB	103	A: 46.12%, G: 53.88%	C: 99.03%, T: 0.97%	0.0115
Japanese in Tokyo, Japan	JPT	104	A: 36.06%, G: 63.94%	C: 100.0%, T: 0.0%	NA
Southern Han Chinese	CHS	105	A: 49.52%, G: 50.48%	C: 100.0%, T: 0.0%	NA
Chinese Dai in Xishuangbanna, China	CDX	93	A: 52.15%, G: 47.85%	C: 99.46%, T: 0.54%	0.005
Kinh in Ho Chi Minh City, Vietnam	KHV	99	A: 53.03%, G: 46.97%	C: 98.48%, T: 1.52%	0.0136
European	EUR	503	A: 95.92%, G: 4.08%	C: 53.78%, T: 46.22%	0.0365
Utah Residents (CEPH) with Northern and Western European Ancestry	CEU	99	A: 95.45%, G: 4.55%	C: 50.51%, T: 49.49%	0.0467
Toscani in Italia	TSI	107	A: 96.73%, G: 3.27%	C: 61.68%, T: 38.32%	0.021
Finnish in Finland	FIN	99	A: 91.92%, G: 8.08%	C: 50.51%, T: 49.49%	0.0862
British in England and Scotland	GBR	91	A: 98.9%, G: 1.1%	C: 43.96%, T: 56.04%	0.0142
Iberian Population in Spain	IBS	107	A: 96.73%, G: 3.27%	C: 60.28%, T: 39.72%	0.0223
South Asian	SAS	489	A: 85.28%, G: 14.72%	C: 79.35%, T: 20.65%	0.0449
Gujarati Indian from Houston, Texas	GIH	103	A: 83.5%, G: 16.5%	C: 80.58%, T: 19.42%	0.0476
Punjabi from Lahore, Pakistan	PJL	96	A: 82.29%, G: 17.71%	C: 81.25%, T: 18.75%	0.0497
Bengali from Bangladesh	BEB	86	A: 83.72%, G: 16.28%	C: 83.14%, T: 16.86%	0.0394
Sri Lankan Tamil from the UK	STU	102	A: 86.76%, G: 13.24%	C: 73.53%, T: 26.47%	0.0549
Indian Telugu from the UK	ITU	102	A: 89.71%, G: 10.29%	C: 78.92%, T: 21.08%	0.0306

Table 3. Genotype distributions of rs12252 and rs34481144 in stratified groups based on symptom burden

RefSNP ID	Associated Allele	Total MAF	Allele Frequency		Genotypes	
			Group 1	**Group 2**	Group 1 (n=29)	Group 2 (n=22)
rs12252 A>G	G	0.078	A: 90 % G: 10 %	A: 95 % G: 5 %	AA (n=20)	AA (n=18)
					AG (n=5)	AG (n=2)
					GG (n=0)	GG (n=0)
					NA (n=4)	NA (n=2)
					x2/*p*-value: 0.775/0.3788	
rs34481144 C>T	T	0.344	C: 66 % T: 34 %	C: 65 % T: 35 %	CC (n=12)	CC (n=8)
					CT (n=9)	CT (n=10)
					TT (n=4)	TT (n=2)
					NA (n=4)	NA (n=2)
					x2/*p*-value: 0.01/0.921	

NA; genotypes not determined, Group 1; individuals who experienced more than 6 COVID-19 symptoms, Group 2; individuals who experienced 6 or less COVID-19 symptoms.

Table 4. Genotype distributions of rs12252 and rs34481144 in individuals stratified based on their COVID post-vaccination (Pfizer-BioNTech) reactions

RefSNP ID	Total MAF	Allele Frequency		Genotypes	
		Group 3	**Group 4**	**Group 3 (n=43)**	**Group 4 (n=104)**
rs12252 A>G	0.126	A: 87.2 % G: 12.8 %	A: 87.4 % G: 12.5%	AA (n=30)	AA (n=73)
				AG (n=8)	AG (n=22)
				GG (n=1)	GG (n=1)
				NA (n=4)	NA (n=8)

				x^2/*p*-value: 0.002/0.9663	
		Group 3	**Group 5**	**Group 3 (n=43)**	**Group 5 (n=14)**
	0.132	A: 87.2 % G: 12.8 %	A: 85.7 % G: 14.3%	AA (n=30) AG (n=8) GG (n=1) NA (n=4)	AA (n=11) AG (n=2) GG (n=1) NA (n=0)
				x^2/*p*-value: 0.039/0.8443	
		Group 3	**Group 6**	**Group 3 (n=43)**	**Group 6 (n=25)**
	0.123	A: 87.2 % G: 12.8 %	A: 88.6 % G: 11.4 %	AA (n=30) AG (n=8) GG (n=1) NA (n=4)	AA (n=17) AG (n=5) GG (n=0) NA (n=3)
				x^2/*p*-value: 0.055/0.814	
rs34481144 C>T		**Group 3**	**Group 4**	**Group 3 (n=43)**	**Group 4 (n=104)**
	0.31	C: 71.3 % T: 28.7 %	C: 68 % T: 32 %	CC (n=20) CT (n=17) TT(n=3) NA (n=3)	CC (n=47) CT (n=39) TT (n=12) NA (n=6)
				x^2/*p*-value: 0.273/0.6016	
		Group 3	**Group 5**	**Group 3 (n=43)**	**Group 5 (n=14)**
	0.352			CC (n=20)	CC (n=3)

	C: 71.3 % T: 28.7 %	C: 46.4 % T: 53.6%	CT (n=17) TT(n=3) NA (n=3)	CT (n=7) TT (n=4) NA (n=0)
			x^2/*p*-value: 5.603/0.0179	
	Group 3	**Group 6**	**Group 3 (n=43)**	**Group 6 (n=25)**
0.312	C: 71.3 % T: 28.7 %	C: 64.56 % T: 35.44 %	CC (n=20) CT (n=17) TT(n=3) NA (n=3)	CC (n=9) CT (n=13) TT (n=2) NA (n=1)
			x^2/*p*-value: 0.621/0.4308	

NA; genotypes not determined,

Group 3; no vaccine reactions.

Group 4; one or more reactions.

Group 5: only local reactions.

Group 6: only systemic reactions.

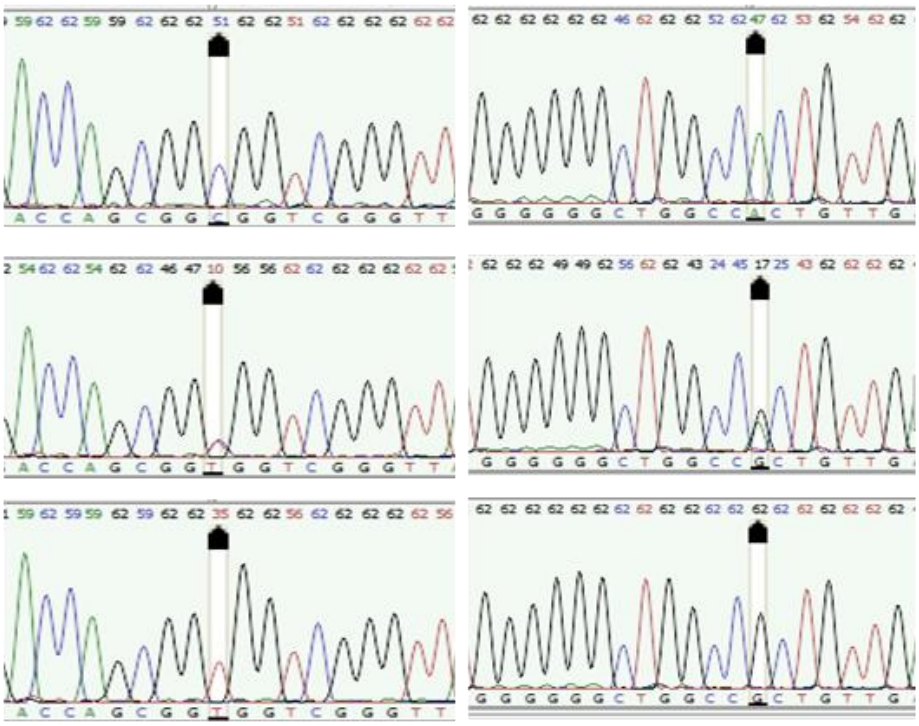

rs34481144 **rs12252**

Figure 1. Sanger Sequencing chromatograms show genotypes obtained for rs12252 and rs34481144

Figure 2. Allele frequency distributions of a) rs12252 and b) rs34481144 in populations across the globe.

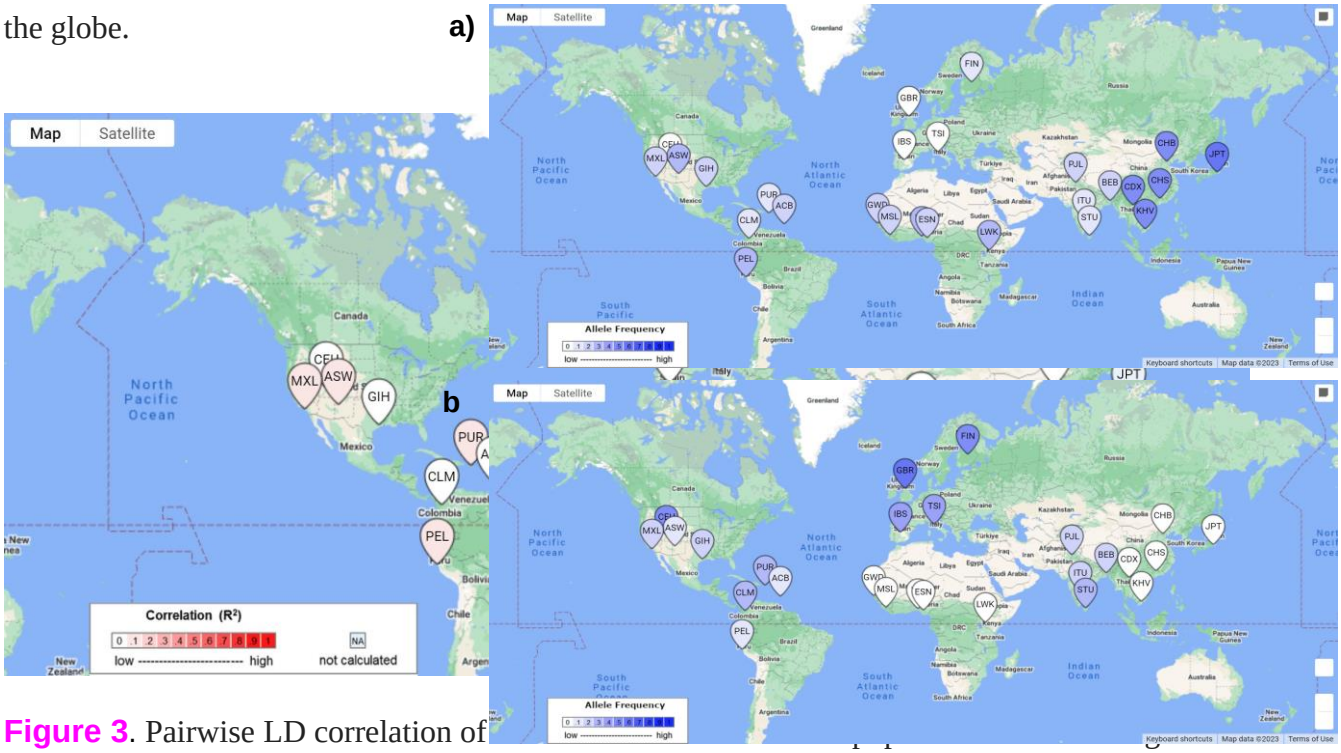

Figure 3. Pairwise LD correlation of

FIGURES

Figure 1. Sanger Sequencing chromatograms show genotypes obtained for a) rs12252 and b) rs34481144

Figure 2. Allele frequency distributions of a) rs12252 and b) rs34481144 in populations across the globe.

Figure 3. Pairwise LD correlations of rs34481144 and rs12252 in populations across the globe.

SUPPLEMENTARY MATERIALS

Supplementary Table 1. Primers used in the Tetra Primer ARMS-PCR protocol

RefSNP ID	Primer	Tm°C	Primer Seq 5'—3'	Flanking Length (bp)	Amplicon Allele Specific Length (bp)	Allele
rs12252A>G	FI	76.1	TCCAAACCTTCTTCTCTCCTGTCAACCGC			G

	RO	76.2	GAAGAGGGTGTTGAACAGGGACCAGACG	280	188	
	FO	76.5	ACCGAAACTACTGGGGAAAGGGAGGGCT		147	A
	RI	76.7	AGCATCTCATAGTTGGGGGGCTGGACA			
rs34481144C>T	FI	76.8	CACTGAGAACCATCCCAGTAACCCGAACG		244	C
	RO	76.8	TGTTGAACAGGGACCAGACGACATGGTC	395		
	FO	76.5	CTTAGCCCTCAGCCCCTCTTTCCTCCCT		209	T
	RI	76.6	CATGGTGTCCAGCGAAGACCAGCTGT			

Supplementary Table 2. Tetra Primer ARMS-PCR conditions for a) rs12252 and b) rs34481144

a)

	Temperature	Time	Cycle
Initial Denaturation	95 ˚C	10 min	
Denature	95 ˚C	15 sec	10
Annealing	70 ˚C -65 ˚C	30 sec	
Extend	72 ˚C	15 sec	
Denature	95 ˚C	15 sec	25
Annealing	65 ˚C	30 sec	
Extend	72 ˚C	15 sec	
Final Extension	72 ˚C	5 min	

b)

	Temperature	Time	Cycle
Initial Denaturation	95 ˚C	10 min	
Denature	95 ˚C	15 sec	10
Annealing	70 ˚C -62 ˚C	30 sec	
Extend	72 ˚C	30 sec	
Denature	95 ˚C	15 sec	25
Annealing	62 ˚C	30 sec	
Extend	72 ˚C	30 sec	
Final Extension	72 ˚C	5 min	

Supplementary Table 3. PCR protocol and conditions used for sequencing the target fragment harboring SNPs

	1X
DNA Template	2–5 µL
10X PCR Buffer	2.5 µL
Mg^{+2}	2 µL
dNTP	0.5 µL
Primers (Forward and Reverse)	0.6 µL from each primer
Nuclease Free Water	16.525–13.525 µL
AmpliTaq Gold Polimerase	0.15 µL
BSA	0.125 µL
Total Volume	25 µL

	Temperature	Time	Cycle
Initial Denaturation	95 ˚C	10 min	
Denature	95 ˚C	15 sec	
Annealing	58 ˚C	30 sec	35–40
Extend	72 ˚C	1 min	
Final Extension	72 ˚C	5 min	

Supplementary Table 4. Sample characteristics and experiences of the COVID-19 pandemic

Age	18–74
Female/Male	123/77
Contacted Status (n)	200
Contacted (n,%)	66 (33.0 %)
Non-contacted (n,%)	134 (67.0 %)
COVID Test Result (n)	200
Non-Tested (n,%)	69 (34.5 %)
Negative (n,%)	65 (32.5 %)
Positive(n,%)	64 (32 %)
Positive and hospitalized (n,%)	2 (1.0 %)
COVID Positive Test Result (n,%)	65
Pre-vaccine Positive (n,%)	35 (53.8 %)
Post-vaccine Positive (n,%)	15 (21.5 %)
Both Pre and Post vaccine Positive (n,%)	16 (24.6 %)
COVID-19 Symptoms / Pre-Vaccine (n)	51
Fever (n, %)	28 (54.9 %)
Chills (n, %)	26 (51.0 %)
Headache (n, %)	30 (58.8 %)
Fatigue (n, %)	41 (80.4 %)
Sore throat (n, %)	27 (52.9 %)
Muscle aches (n, %)	31 (60.8 %)
Loss of Smell (n, %)	27 (52.9 %)
Loss of Taste(n, %)	28 (54.9 %)
Diarrhea (n, %)	9 (17.6 %)
Shortness of Breath (n, %)	12 (23.5 %)
Cough (n, %)	27 (52.9 %)
Congestion or runny nose (n, %)	26 (51.0 %)
Vaccine Status (n)	200
Not vaccinated	7 (3.5 %)
Pfizer-BioNTech	147 (73.5 %)
Sinovac	24 (11.5 %)
Pfizer-BioNTech + Sinovac	20 (10 %)
Pfizer-BioNTech + Turkovac	1 (0.5 %)
Pfizer-BioNTech + Moderna	1 (0.5 %)
Vaccine Reactions	
No Reactions (n, %)	63 (32.7 %)
Pain at the injection site (n, %)	98 (50.8 %)
Redness at the injection site (n, %)	15 (7.8 %)
Swelling at the injection site (n, %)	23 (11.9 %)
Fever (n, %)	45 (32.3 %)
Fatigue (n, %)	77 (39.9 %)
Headache (n, %)	52 (26.9 %)
Chills (n, %)	17 (8.8 %)
Tiredness (n, %)	69 (35.8 %)

Vomit (n, %)	6 (3.1 %)
Diarrhea (n, %)	7 (3.6 %)
Muscle aches (n, %)	61 (31.6 %)
Joint Pain (n, %)	39 (20.2 %)
Low Sugar (n, %)	10 (5.2 %)
Abdominal Pain (n, %)	5 (2.6 %)
Fainting (n, %)	5 (2.6 %)
Increased Heart Rhythm (n, %)	14 (7.3 %)
Difficulty Breathing (n, %)	8 (4.1 %)
Hives (n, %)	2 (1.0 %)

Supplementary Table 5. rs34481144 and rs12252 retrieved from RegulomeDB and Genotype-Tissue Expression (GTEx) databases

RefSNP ID	RegulomeDB	eQTL	*p*-Value	NES *	Tissue
rs12252	1f	*PGGHG*	0.000022	-0.36	Lung
			0.000027	-0.48	Brain—Frontal Cortex (BA9)
			0.00010	-0.31	Muscle—Skeletal
			0.00013	-0.42	Adipose—Subcutaneous
			0.00014	-0.25	Skin—Sun Exposed (Lower leg)
		RP11–326C3.13	0.000030	-0.54	Nerve—Tibial
		RP11–326C3.15	0.000036	-0.30	Whole Blood
		RP11–326C3.2	0.000053	-0.35	Lung
rs34481144	1f	*IFITM1*	3.0e-13	0.21	Nerve—Tibial
			3.2e-10	0.18	Esophagus—Muscularis
			1.2e-9	0.17	Thyroid
			4.6e-9	0.15	Testis
			7.9e-9	0.14	Muscle—Skeletal
			8.8e-9	0.13	Skin—Sun Exposed (Lower leg)
			2.3e-8	0.22	Heart—Atrial Appendage
			3.9e-7	0.16	Adipose—Visceral (Omentum)
			0.0000011	0.19	Brain—Nucleus accumbens (basal ganglia)
			0.0000012	0.11	Skin—Not Sun Exposed (Suprapubic)
			0.0000014	0.18	Esophagus—Gastroesophageal Junction
			0.0000015	0.18	Artery—Aorta
			0.0000021	0.091	Whole Blood
			0.0000024	0.14	Heart—Left Ventricle
			0.0000026	0.32	Adrenal Gland
			0.0000032	0.33	Ovary
			0.0000050	0.22	Pancreas
			0.0000086	0.14	Lung
			0.000012	0.11	Artery—Tibial
			0.000019	0.17	Brain—Cortex
			0.000021	0.16	Colon—Sigmoid
			0.000028	0.098	Adipose—Subcutaneous
			0.000042	0.12	Cells—Cultured fibroblasts
			0.000053	0.11	Esophagus—Mucosa
		IFITM2	3.5e-11	0.23	Cells—Cultured fibroblasts
			4.0e-8	0.60	Cells—EBV-transformed lymphocytes
			0.000063	0.12	Esophagus—Muscularis
			0.00019	0.12	Artery—Tibial
		IFITM3	4.1e-52	-0.54	Whole Blood
			1.0e-23	-0.25	Testis
			5.2e-14	-0.25	Pancreas
			2.6e-13	-0.17	Nerve—Tibial
			6.7e-13	-0.25	Brain—Putamen (basal ganglia)

			8.1e-13	-0.16	Esophagus—Mucosa
			2.4e-12	-0.15	Skin—Not Sun Exposed (Suprapubic)
			3.2e-12	-0.22	Brain—Caudate (basal ganglia)
			7.8e-12	-0.15	Breast—Mammary Tissue
			2.5e-11	-0.26	Brain—Hypothalamus
			2.6e-11	-0.23	Brain—Cortex
			2.4e-10	-0.12	Skin—Sun Exposed (Lower leg)
			2.7e-10	-0.23	Brain—Nucleus accumbens (basal ganglia)
			2.9e-10	-0.13	Adipose—Subcutaneous
			3.9e-9	-0.14	Thyroid
			8.2e-9	-0.10	Colon—Transverse
			2.1e-7	-0.29	Brain—Substantia nigra
			2.9e-7	-0.52	Cells—EBV-transformed lymphocytes
			7.7e-7	-0.11	Lung
			0.0000015	-0.11	Adipose—Visceral (Omentum)
			0.0000020	-0.10	Muscle—Skeletal
			0.0000024	-0.13	Colon—Sigmoid
			0.0000048	-0.18	Brain—Cerebellum
		PGGHG	1.5e-7	0.23	Esophagus—Muscularis
			4.5e-7	0.22	Nerve—Tibial
			0.0000017	0.26	Brain—Caudate (basal ganglia)
			0.0000020	0.27	Brain—Hypothalamus
			0.0000030	0.23	Colon—Sigmoid
			0.0000045	0.32	Brain—Cerebellar Hemisphere
			0.0000084	0.17	Muscle—Skeletal
			0.000016	0.18	Artery—Tibial
			0.000021	0.29	Brain—Cerebellum
			0.000032	0.13	Skin—Not Sun Exposed (Suprapubic)
			0.000066	0.17	Lung
			0.00015	0.19	Adipose—Subcutaneous
			0.00020	0.12	Skin—Sun Exposed (Lower leg)
		RP11–326C3.11	1.8e-25	-0.50	Adipose—Subcutaneous
			5.8e-24	-0.46	Skin—Sun Exposed (Lower leg)
			1.5e-19	-0.46	Skin—Not Sun Exposed (Suprapubic)
			2.2e-17	-0.47	Breast—Mammary Tissue
			1.5e-10	-0.33	Artery—Tibial
			4.9e-9	-0.38	Brain—Nucleus accumbens (basal ganglia)
			1.1e-8	-0.38	Esophagus—Gastroesophageal Junction
			4.9e-8	-0.54	Minor Salivary Gland
			7.5e-8	-0.42	Brain—Putamen (basal ganglia)
			1.0e-7	-0.36	Brain—Caudate (basal ganglia)
			1.4e-7	-0.29	Artery—Aorta
			1.6e-7	-0.32	Stomach
			1.8e-7	-0.27	Colon—Transverse
			5.5e-7	-0.24	Thyroid
			6.2e-7	-0.23	Lung
			8.2e-7	-0.14	Whole Blood
			0.0000038	-0.23	Muscle—Skeletal
			0.000021	-0.37	Spleen
			0.000026	-0.38	Brain—Spinal cord (cervical c-1)
			0.000036	-0.19	Adipose—Visceral (Omentum)
			0.00017	-0.20	Esophagus—Muscularis
		RP11–326C3.12	2.2e-55	0.93	Esophagus—Muscularis
			8.5e-34	0.80	Colon—Sigmoid
			6.7e-33	0.63	Artery—Tibial
			3.8e-32	0.82	Esophagus—Gastroesophageal Junction
			1.4e-30	0.63	Nerve—Tibial
			4.7e-30	0.88	Brain—Caudate (basal ganglia)
			6.9e-28	0.81	Brain—Nucleus accumbens (basal ganglia)
			8.7e-27	0.89	Brain—Putamen (basal ganglia)
			2.4e-26	0.82	Brain—Hypothalamus
			1.1e-23	0.73	Brain—Cortex
			3.5e-23	0.79	Brain—Cerebellum
			6.8e-21	0.61	Artery—Aorta
			1.4e-20	0.82	Brain—Amygdala
			3.4e-19	0.87	Brain—Substantia nigra
			4.4e-19	0.77	Brain—Hippocampus
			7.6e-19	0.43	Skin—Sun Exposed (Lower leg)
			8.4e-19	0.54	Testis

			1.6e-18	0.78	Brain—Anterior cingulate cortex (BA24)
			4.6e-18	0.68	Brain—Frontal Cortex (BA9)
			9.5e-18	0.79	Prostate
			5.4e-17	0.69	Brain—Cerebellar Hemisphere
			1.0e-15	0.48	Colon—Transverse
			7.5e-15	0.82	Brain—Spinal cord (cervical c-1)
			5.1e-14	0.41	Skin—Not Sun Exposed (Suprapubic)
			9.2e-12	0.37	Esophagus—Mucosa
			3.7e-11	0.46	Stomach
			2.6e-9	0.21	Whole Blood
			2.8e-9	0.51	Liver
			3.9e-9	0.29	Thyroid
			4.5e-9	0.56	Adrenal Gland
			5.4e-9	0.32	Adipose—Subcutaneous
			9.0e-9	0.37	Breast—Mammary Tissue
			1.3e-8	0.47	Pancreas
			1.6e-8	0.27	Lung
			2.4e-8	0.39	Pituitary
			0.0000010	0.29	Adipose—Visceral (Omentum)
		RP11–326C3.13	2.3e-54	0.62	Whole Blood
			4.7e-32	0.70	Nerve—Tibial
			3.7e-18	0.44	Artery—Tibial
			7.4e-18	0.65	Colon—Sigmoid
			2.9e-16	0.45	Lung
			6.6e-16	0.61	Esophagus—Gastroesophageal Junction
			1.7e-15	0.52	Esophagus—Muscularis
			2.3e-12	0.42	Testis
			1.1e-11	0.36	Skin—Sun Exposed (Lower leg)
			1.2e-11	0.45	Breast—Mammary Tissue
			1.4e-11	0.48	Artery—Aorta
			1.3e-10	0.46	Stomach
			2.2e-10	0.38	Adipose—Subcutaneous
			3.3e-10	0.45	Colon—Transverse
			3.3e-10	0.34	Thyroid
			5.1e-10	0.30	Adipose—Visceral (Omentum)
			5.3e-9	0.40	Heart—Left Ventricle
			1.3e-7	0.47	Brain—Nucleus accumbens (basal ganglia)
			1.5e-7	0.39	Pituitary
			1.9e-7	0.48	Artery—Coronary
			3.0e-7	0.42	Spleen
			4.2e-7	0.59	Ovary
			0.0000028	0.32	Heart—Atrial Appendage
			0.000018	0.41	Brain—Frontal Cortex (BA9)
			0.000033	0.23	Cells—Cultured fibroblasts
		RP11–326C3.14	8.4e-19	0.59	Testis
		RP11–326C3.15	6.4e-20	0.49	Nerve—Tibial
			1.5e-17	0.64	Brain—Nucleus accumbens (basal ganglia)
			3.9e-17	0.64	Brain—Caudate (basal ganglia)
			4.7e-15	0.66	Brain—Anterior cingulate cortex (BA24)
			5.0e-14	0.52	Colon—Sigmoid
			7.4e-14	0.36	Artery—Tibial
			8.9e-14	0.26	Whole Blood
			2.0e-11	0.61	Brain—Putamen (basal ganglia)
			3.3e-11	0.70	Brain—Amygdala
			9.0e-11	0.51	Brain—Hypothalamus
			2.4e-9	0.50	Liver
			2.5e-9	0.32	Esophagus—Muscularis
			5.9e-9	0.55	Prostate
			1.1e-8	0.45	Brain—Cerebellum
			2.9e-8	0.36	Brain—Cortex
			3.0e-8	0.35	Colon—Transverse
			3.2e-8	0.36	Esophagus—Gastroesophageal Junction
			3.7e-8	0.36	Artery—Aorta
			9.3e-8	0.50	Brain—Hippocampus
			2.1e-7	0.36	Testis
			2.4e-7	0.25	Skin—Sun Exposed (Lower leg)
			4.4e-7	0.23	Lung
			4.9e-7	0.52	Brain—Substantia nigra

			5.2e-7	0.40	Brain—Frontal Cortex (BA9)
			0.000034	0.21	Skin—Not Sun Exposed (Suprapubic)
			0.000078	0.33	Brain—Cerebellar Hemisphere
		RP11–326C3.7	6.4e-16	0.29	Artery—Tibial
			3.0e-15	0.32	Whole Blood
			3.0e-7	0.53	Cells—EBV-transformed lymphocytes
			3.0e-7	0.21	Thyroid
			0.0000026	0.36	Brain—Substantia nigra
			0.0000040	0.25	Esophagus—Gastroesophageal Junction
			0.000012	0.18	Breast—Mammary Tissue
			0.000016	0.20	Colon—Transverse

*Normalized Effect Size, 1f: eQTL/caQTL + TF binding / chromatin accessibility peak